Ocean Dynamics (2011) 61:807–827
DOI 10.1007/s10236-011-0395-6

Future wave climate over the west-European shelf seas

Anna Zacharioudaki · Shunqi Pan · Dave Simmonds · Vanesa Magar · Dominic E. Reeve

Received: 26 January 2010 / Accepted: 14 February 2011 / Published online: 6 April 2011

Abstract In this paper, we investigate changes in the wave climate of the west-European shelf seas under global warming scenarios. In particular, climate change wind fields corresponding to the present (control) time-slice 1961–2000 and the future (scenario) time-slice 2061–2100 are used to drive a wave generation model to produce equivalent control and scenario wave climate. Yearly and seasonal statistics of the scenario wave climates are compared individually to the corresponding control wave climate to identify relative changes of statistical significance between present and future extreme and prevailing wave heights. Using global, regional and linked global–regional wind forcing over a set of nested computational domains, this paper further demonstrates the sensitivity of the results to the resolution and coverage of the forcing. It suggests that the use of combined forcing from linked global and regional climate models of typical resolution and coverage is a good option for the investigation of relative wave changes in the region of interest of this study. Coarse resolution global forcing alone leads to very similar results over regions that are highly exposed to the Atlantic Ocean. In contrast, fine resolution regional forcing alone is shown to be insufficient for exploring wave climate changes over the western European waters because of its limited coverage. Results obtained with the combined global–regional wind forcing showed some consistency between scenarios. In general, it was shown that mean and extreme wave heights will increase in the future only in winter and only in the southwest of UK and west of France, north of about 44–45° N. Otherwise, wave heights are projected to decrease, especially in summer. Nevertheless, this decrease is dominated by local wind waves whilst swell is found to increase. Only in spring do both swell and local wind waves decrease in average height.

Keywords Climate change · Wave climate scenarios · North Atlantic · Western Europe

Abbreviations

AGCM	Atmospheric Global Climate Model
AR4	Assessment Report 4
CERA	Climate and Environmental Retrieval and Archive
CLM	Climate Local Model
ECHAM5	5th Generation of Global Climate Model developed by the Max Planck Institute for Meteorology
ETOP01	1 arc-minute global relief model of Earth's surface that integrates land topography and ocean bathymetry
GCM	Global Climate Model
GEV	Generalized Extreme Value
IPCC	Intergovernmental Panel on Climate Change
MPI-M	Max Planck Institute for Meteorology
NCEP	National Centers for Environmental Prediction

Responsible Editor: Roger Proctor

A. Zacharioudaki (✉)
CIMA - Centre for Marine and Environmental Research,
University of the Algarve,
Hidrotec-ISE, Campus da Penha,
Faro 8005-139, Portugal
e-mail: azzacharioudaki@ualg.pt

S. Pan · D. Simmonds · V. Magar · D. E. Reeve
Coastal Engineering Research Group,
School of Marine Science and Engineering,
University of Plymouth,
Drake Circus,
Plymouth, Devon PL4 8AA, UK

NGDC	National Geophysical Data Center
NOAA	National Oceanic and Atmospheric Administration
RCM	Regional Climate Model
RLP	Return Level Plot
SLP	Sea Level Pressure
SRES	Special Report on Emissions Scenarios
STOWASUS-2100	Research Project: regional STOrm WAve and SUrge Scenarios for the 2100 century
SWRDA	South West Regional Development Agency UK
UKCIP	UK Climate Impacts Programme
WAM	WAve Model
WAMDI	Work Group for WAM model
WASA	Research Project: Waves and Storms in the North Atlantic
WDCC	World Data Center for Climate
WMO	World Meteorological Organization
WW3	Wave Watch III model

1 Introduction

Statistical knowledge of deep water wave climate is extremely important in several fields. Offshore, ships and structures are designed using criteria based on the known statistics of those waves they are expected to encounter. On the coast, the predicted performance of man-made sea defences such as sea walls and natural sea defences such as beaches, are stated in terms of the return period of extreme wave heights and water levels. The occurrence of such extremes is intrinsically linked to the statistics of the wave climate offshore through the well-understood science of wave transformation modelling. More recently, a good understanding of regional wave climate has proven essential for the design, development, planning and operation of marine renewable energy devices. Again, the wave statistics are used to characterise the wave resource and to determine the design criteria for survivability. Indeed, there is much focus for wave energy research on the west-European shelf seas from UK, Portugal and Spain.

Knowledge of the present day wave climate and its potential future changes as a result of global warming are equally important for sustainable planning and design. Investigations of such changes have become possible with the development of more robust climate models in the 1990s. By the dawn of the twenty-first century, a growing amount of data from Global Climate Models (GCMs) at coarse resolution and Regional Climate Models (RCMs) at a higher resolution has been made publicly available for use in impact assessment studies and policy-making. Using such data, specifically wind fields and/or sea level pressure (SLP) fields, a number of studies of different spatial coverage and resolution have been used to predict future wave climates.

The WASA project (WASA 1998) was the first study to assess changes between future and present wave conditions over the north-northeast Atlantic and the North Sea. A climate change time-slice experiment was performed with the use of a GCM. However, the length of the control (present) and scenario (future) simulations were only 5 years and the changes found fell well within the limits of natural variability. The WASA project was followed by the STOWASUS-2100 project (Kaas et al. 2001) which used longer simulation to assess future changes in wave conditions around Europe and the North Atlantic. In their project, wind fields from a 30-year time-slice climate change experiment carried out with a GCM and for a single greenhouse gas emissions scenario, were used to drive the wave model WAM (WAMDI 1988) to generate the corresponding wave fields. Amongst the findings were a projected decrease in both the mean and extremes of significant wave height, H_s, at west and southwest of the British Isles but a general increase in these quantities in the North Seas. Wang et al. (2004), Wang and Swail (2006) and Caires et al. (2006) reported subsequent studies that used empirical downscaling methods relating seasonal mean SLP from GCMs to H_s. In these studies they analysed seasonal trends in mean and extreme H_s using data for a continuous interval of time from the present. Three forcing scenarios—each of them represented by an ensemble of three realisations—were used in the analysis. A particular feature of the Wang and Swail (2006) study was the implementation of a multi-model approach. In general, results from these studies showed that uncertainties due to different emissions scenarios, although often significant, were smaller than uncertainties caused by use of alternate GCMs. Nevertheless, the multi-model projections of climate change showed similar patterns—albeit with some regional differences—to those derived from a single GCM. Furthermore, the forcing-induced variance, i.e. that variance attributed entirely to differences in the internal model variability (which is an imperfect replica of the natural variability) between different climate realisations of the same forcing scenario, was found significant for some parts of the globe. To the west of the North Sea in the North Atlantic and away from the tropics, however, this uncertainty was relatively small. Debernard et al. (2002) dynamically downscaled GCM projections to a 55-km resolution over Northern Europe and adjacent parts of the North Atlantic Ocean, using a RCM. The extended study of Debernard et al. (2008), based on 30-year long time-slices, considered three emissions scenarios and used a multi-model approach that incorporated three GCMs. In agreement with the previous work, they found considerable model-induced uncertainty in the results. However, they also found that the majority of their climate change experiments showed a significant increase in the annual

99 percentile of H_s (a statistical measure of the extremes) and its winter mean west and southwest of the British Isles. Similar analyses were carried out by Grabemann and Weisse (2008) for the North Sea and by Kriezi and Broman (2008) for the Baltic Sea.

An issue related to the quality of the results of the aforementioned studies is the appropriate consideration of the swell component of the wave climate. In particular, swell propagation from the greater north Atlantic Ocean can play a major role in shaping the wave climate of the southwest of UK (e.g. Hawkes et al. 1997) and also west France, Spain and Portugal, i.e. what is referred to as the west-European shelf seas in the present study. The work by Bouws et al. (1997) and Gulev and Hasse (1999) found that wave height increases observed in recent decades over the North Atlantic are connected with growing swell rather than wind sea waves. The latter actually shows significant negative trends over time in the 50 and higher percentile exceedances. Therefore, any conclusions on the wave climate over the west-European shelf seas drawn from model results which exclude a great part of the North Atlantic are likely to be inaccurate and should be used with caution. Specifically, waves generated west of ~30° W and south of ~40° N have been ignored in those above-mentioned studies which employed wind-driven wave generation models. Nevertheless, wave propagation from northern sectors has been well represented in those studies. As a result, over the North and Baltic Seas where swell propagation from the area of the Atlantic Ocean situated west of the British Isles is of minor importance, the reported future wave changes should represent changes in the complete wave spectrum.

Although Wang and Swail (2006) and Caires et al. (2006) used a global domain, their statistical downscaling approach has an important disadvantage; the basic assumption of the method, i.e. the assumption that the statistical relationship established for the present will hold unchanged in the future, is not verifiable (Fowler et al. 2007). It is only recently that Lowe et al. (2009) explicitly considered the impact of swell on the changes of the wave climate in the North Atlantic between present and future. Their study, widely known as UKCIP09, applied a nested set of WAM models consisting of a 1×1° horizontal resolution domain covering the whole of the Atlantic Ocean and a 12×12 km nested domain covering the northwest-European continental shelf. Surface winds from GCM–RCM climate change experiments were used to force the wave model. The GCM winds forced the coarse resolution domain whilst the RCM winds forced the finer resolution nested domain, thereby accounting for the propagation of swell from distant locations into the finer grid. Relative changes between present and future wave conditions were investigated for an intermediate emissions scenario. It was shown that swell dominates the seasonal mean H_s, especially in spring and summer.

In addition, UKCIP09 aimed to enhance the results near the coast by accounting for the small to medium-scale phenomena occurring in this region (e.g. land-sea breezes, orographic effect and fronts), not captured by the coarse resolution of GCMs. This is why RCM wind fields were used to force the nested WAM domain. The increased resolution of RCMs, able to resolve mesoscale phenomena, is thought to lead to the enhanced simulation of climate variability and extremes in the nearshore zone, and possibly in a better representation of the overall wind climate (e.g. Mearns et al. 1997; Kaas and Andersen 2000; IPCC AR4 2007). Recently, Sotillo et al. (2005) and Winterfeldt and Weisse (2009) explicitly quantified the agreement between surface wind speeds obtained from RCMs forced by global reanalysis output (e.g. output from a GCM which assimilates quality controlled data), the global reanalysis winds and measurements over the Northeast Atlantic and/or the Mediterranean Sea. A technique that keeps the RCM solution close to that of the global reanalysis for larger scales that are well supported by data assimilation was in place. The aim was to assess whether RCM winds do indeed show an added value in comparison to the global reanalysis winds. Combining the results of the two studies it can be stated that, in general, the instantaneous global reanalysis wind speeds are enhanced after RCM downscaling in coastal areas and particularly those that are characterised by increased orographic complexity. Even if the enhancement in instantaneous wind speeds at coastal locations is minor, their frequency distribution and interannual variability is more noticeably enhanced and extreme events are better represented. Also, the possibility for an improved representation of the directional distribution of wind exists (Sotillo et al. 2005). On the other hand, no enhancement of global wind fields through dynamical downscaling was found for open ocean locations, where large-scale processes dominate. Considering other climatic variables or domains, similar results were obtained from Castro et al. (2005) and Feser (2006). It should be noted that Winterfeldt and Weisse (2009) state that the meaning of their results for climate change simulations is unclear. We would argue that the finding that the frequency distribution and interannual variability always improves at coastal locations is very important for climate change assessments in the coastal zone. This is because climate change assessments, including UKCIP09 and the present work, primarily base their conclusions on statistical measures that compare the future interannual variability of a climatic variable to its present variability; the accuracy with which the present wave climate is simulated, is less important. In conclusion, the use of wind forcing from a GCM–RCM combination by UKCIP09 is

believed to have resulted to an improved analysis of a changing wave climate near the coast, compared with a situation when GCM wind output alone is used as forcing.

The study reported here investigates future changes in the North Atlantic wave climate under three emissions scenarios, focusing on the west-European shelf seas between 37° and 52° N. As demonstrated in UKCIP09, due consideration of swell is made in the present study. Relative changes in the mean annual and mean seasonal values of H_s are examined by comparing the results over two time-slices. These time-slices cover the 'present' (1961–2000) conditions, regarded as the 'control' conditions and a century later into the 'future' conditions (2061–2100). Changes in extreme values are also explored. Following UKCIP09, the present study also uses the wind data from a GCM–RCM combination to force a nested wave model.

However, there are some significant differences and additions in the work here. The GCM–RCM combination, the wave model and the wave model set-up are different to those in UKCIP09. In order to better account for the effects of bathymetry on the wave characteristics, this study uses four nested computational domains of the WAVEWATCH III wave model (Tolman 2002a). Furthermore, the finer resolution nested domain, forced with the high resolution RCM data, extends further south to the Strait of Gibraltar. As a result, wave climate variability and extremes should be better captured along most of the west-European continental shelf. In this study, additional greenhouse gas emissions scenarios and longer time-slices are used and an analysis of the statistical significance of the changes is presented. The work is also extended to explore the sensitivity of the results to two aspects of the methodology: (1) omission of the wave modelling domain forced by the GCM data, i.e. omission of distant swell; (2) omission of RCM forcing data, i.e. use of GCM forcing alone throughout the analysis. The former sensitivity analysis demonstrates the impact of implementing 'typical' RCM output alone instead of the GCM–RCM combination on the relative changes between control and scenario. By 'typical', we mean publicly available RCM experiments having a typical coverage (~11° W–37° E and 35–70° N) and resolution (12–50 km). The former analysis also evaluates the inadequacy of 'typical' RCM simulations for climate change wave impact assessment studies at regions exposed to the open ocean, i.e. the North Atlantic in this case. The latter analysis is used to identify the circumstances under which GCM forcing alone might be sufficient. It is assumed that the use of GCM–RCM combination forcing improves the estimates of relative changes between present and future wave climates at the regional scale. However, at locations far away from the coast, this might not be the case (Winterfeldt and Weisse 2009).

This study focuses on the improvement of knowledge concerning the likely changes to wave climate over the next century in an area of the European continental shelf where this is currently poorly understood.

The paper is laid out as follows: the modelling methodology and details of data sets used are described in section 2; section 3 presents results of the annual and seasonal wave statistics along with a detailed analysis of the extremes at selected locations; the paper closes with a discussion in section 4.

2 Methodology

2.1 Atmospheric climate data

The climate change wind scenarios used in this study are produced from climate change experiments performed by the MPI-M and are available through the WDCC/CERA database (WDCC 2009). They are generated by two climate models: the ECHAM5 AGCM at 1.875×1.875° horizontal resolution (Roeckner et al. 2003) and the CLM–RCM at 0.2×0.2° horizontal resolution (Hollweg et al. 2008) driven by ECHAM5. These are state-of-the art models that have been found to have a good skill (e.g. IPCC AR4 2007; van Ulden and van Oldenborgh 2006; van Ulden et al. 2007) and, in general, to perform similarly to other climate models in terms of a number of variables (e.g. sea-surface temperature, precipitation, large-scale circulation). ECHAM5 global winds are at six-hourly intervals whilst CLM regional winds are hourly. Data used herein cover two 40-year time-slices, the 'present' or 'control' period, 1961–2000, and the future or 'scenario' period, 2061–2100. Data from 1960 was used for sensitivity testing. Three IPCC greenhouse gas emissions scenarios (IPCC SRES 2000; IPCC AR4 2007) are examined in this study: B1, A1B and A2, which is available only from ECHAM5. Scenario B1 is associated with a substantial decrease in gas emissions after 2040, reaching levels below those at 2000 by the end of the twenty-first century. It is referred as a 'low-emissions' scenario. Scenario A2 is associated with a rapid increase in greenhouse gas emissions to 2100. This is a 'high-emissions' scenario. Scenario A1B is an intermediate level of greenhouse gas emissions between B1 and A2 and is referred as a 'medium–high-emissions' scenario.

2.2 Wave model set-up

The wind data from each climate change scenario is used to drive the state-of-the art WAVEWATCH III (WW3) v2.22 spectral wave model and generate a corresponding wave field. The WW3 model is the operational wave model of

the American National Centres for Environmental Predictions (NCEP/NOAA) and has been extensively validated (e.g. Cardone et al. 1996; Tolman 2002b; Hanson et al. 2009). In comparison with WAM, WW3 has been found to better capture the wave height variability in regions where swell is generated nearby (Padilla-Hernández et al. 2004; NCEP 2006). Also, it includes sub-grid representation of unresolved islands (Tolman 2003) which leads to improved estimates of depth-induced refraction or blockage of wave energy. It is thus possible that the sensitivities to changes in the input wind fields are different in WAM and WW3.

Figure 1 shows the wave model set-up. The outer computational domain, denoted as N1, covers the north Atlantic from 67° to 2° W and from 28° to 65° N at grid resolution of 0.8° square. Three one-way nested computational domains of finer resolutions, approaching the west-European shelf seas, are embedded within N1, namely: N2 with a medium resolution of 0.4°, and the progressively smaller two domains, N3 and N4 both having the finest resolution of 0.2°. Table 1 provides full details of their coverage. The western boundary of N4 was chosen to coincide with the westernmost boundary of the 0.2°CLM regional wind data, thus allowing forcing of this domain at an identical grid resolution. Outside N4, only the coarser ECHAM5 global winds were used. The bathymetry data was obtained from the ETOPO1 data (NGDC 2009) at 1 arc-minute resolution (≈0.016°). Obstruction grids were generated as described in Chawla and Tolman (2007). Propagation time steps were set to 1 h for the coarse and medium grids and 0.5 h for the fine grids. Input winds were linearly interpolated in time. The calculated wave parameters were output at each grid point at 3-h intervals.

The extent of the outer domain N1 was defined on the basis of good representation of swell and also computational efficiency and data storage. To test this choice, the sensitivity of the output at several points along the eastern Atlantic approach, within N4, was studied against the progressive reduction of an initially very large domain covering the whole of the North Atlantic Ocean. GCM wind forcing corresponding to the winter season of 1960 was used for this sensitivity test. The N1 domain as illustrated was found to be optimal, with differences between this and the largest domain held below 3% for all modelled mean wave parameters. Differences were found to be particularly sensitive to movement of the western boundary, rather than the northern and southern boundaries, indicating the importance of the Northern Atlantic fetch for swell in the western approaches to Europe.

2.3 Sensitivity tests

The use of a large computational domain at a high spatial resolution (e.g. N1 at 0.2° resolution) is expected to provide the best possible results as it properly accounts for the swell component but also it well resolves the underlying bathymetry. However, this approach is very computationally demanding for long-term simulations. On the other hand, the alternative approach of using nested domains of progressively finer resolution can reach similar accuracy but at substantially reduced computing time. Nevertheless, achieving the required accuracy at the desired computational time is not straightforward and an optimal composition of domains and resolutions needs to be tested. Here, to design the nested grids, a benchmark simulation at 0.2° resolution was performed over the whole N1 domain, forced by spatially and temporally interpolated ECHAM5 wind fields from January 1960. This was compared with the results obtained by combining nested domains with different resolutions and/or extents but the

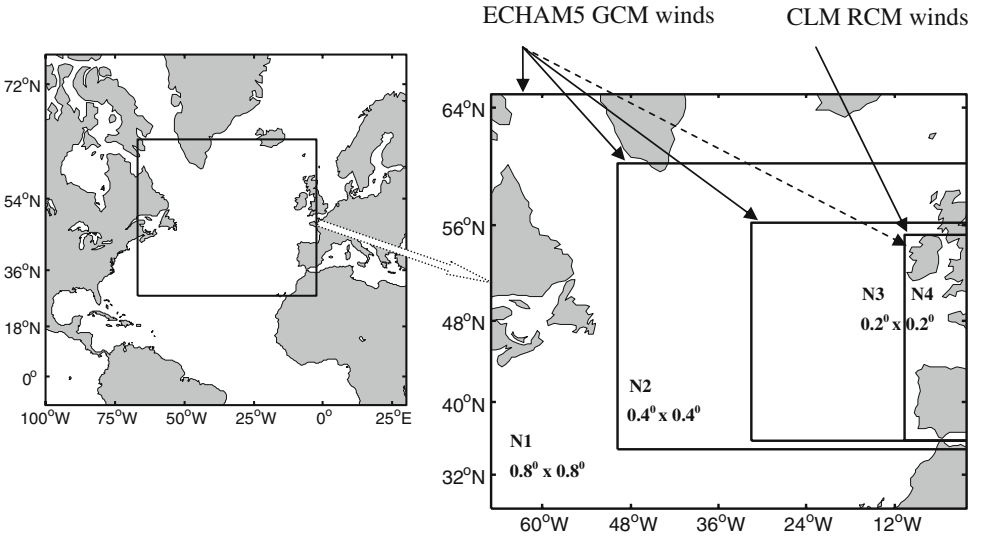

Fig. 1 Grid definition for four one-way nested computational domains (N1, N2, N3 and N4). The wind forcing for each computational domain is indicated. Wave simulations over fine grid resolution domain N4 were forced with both GCM and RCM winds

Table 1 Bathymetry grid definitions

Grid	Grid spacing (longitude×latitude)	South	North	West	East
N1, coarse	0.8×0.8°	28°	64.8°	67°	−2.2°
N2, medium	0.4×0.4°	34.8°	60.4°	49.8°	−2.6°
N3, fine 1	0.2×0.2°	35.8°	56.2°	31.6°	−2.8°
N4, fine 2	0.2×0.2°	35.8°	55.2°	10.6°	−2.8°

same overall extent. Comparisons focused on the values in the Eastern Atlantic Approach were used to find an optimal nesting which produced results close to the benchmark, i.e. a nesting that sufficiently resolved important bathymetric features and was computationally affordable.

Figure 2a shows the maximum absolute percentage differences between hourly H_s values obtained from the benchmark simulation and those from the nested N1, N2 and N3 grids driven by ECHAM5 winds. The maximum differences do not exceed 8% over the area of interest which was considered to be a very good performance.

Figure 2b shows percentage (b1) and absolute H_s differences (b2) between the benchmark and a simulation when domain N4 is forced with CLM–RCM winds instead of the ECHAM5 GCM data. In this case the boundary wave conditions are provided by the benchmark. The high sensitivity of the output to the spatial and temporal resolution of the forcing is evident in this figure. Specifically, it can be seen that the differences range from about 20–25% (0.2–0.8 m) off the Portuguese coast to 90% (0.8–2 m) or greater over the southwest of UK, west of Brittany and north of Spain. Greater difference, >90% and greater than 2 m, are also present in the Irish Sea, and those areas of the English Channel and of the Strait of Gibraltar included within the domain. These may be attributed to the more complex orography and land-sea distribution of these regions. The greatest benefit from RCM downscaling within the English Channel and the Strait of Gibraltar agrees well with the findings of Winterfeldt and Weisse (2009) for the Northeast Atlantic north of about 47° N, and Sotillo et al. (2005) for the

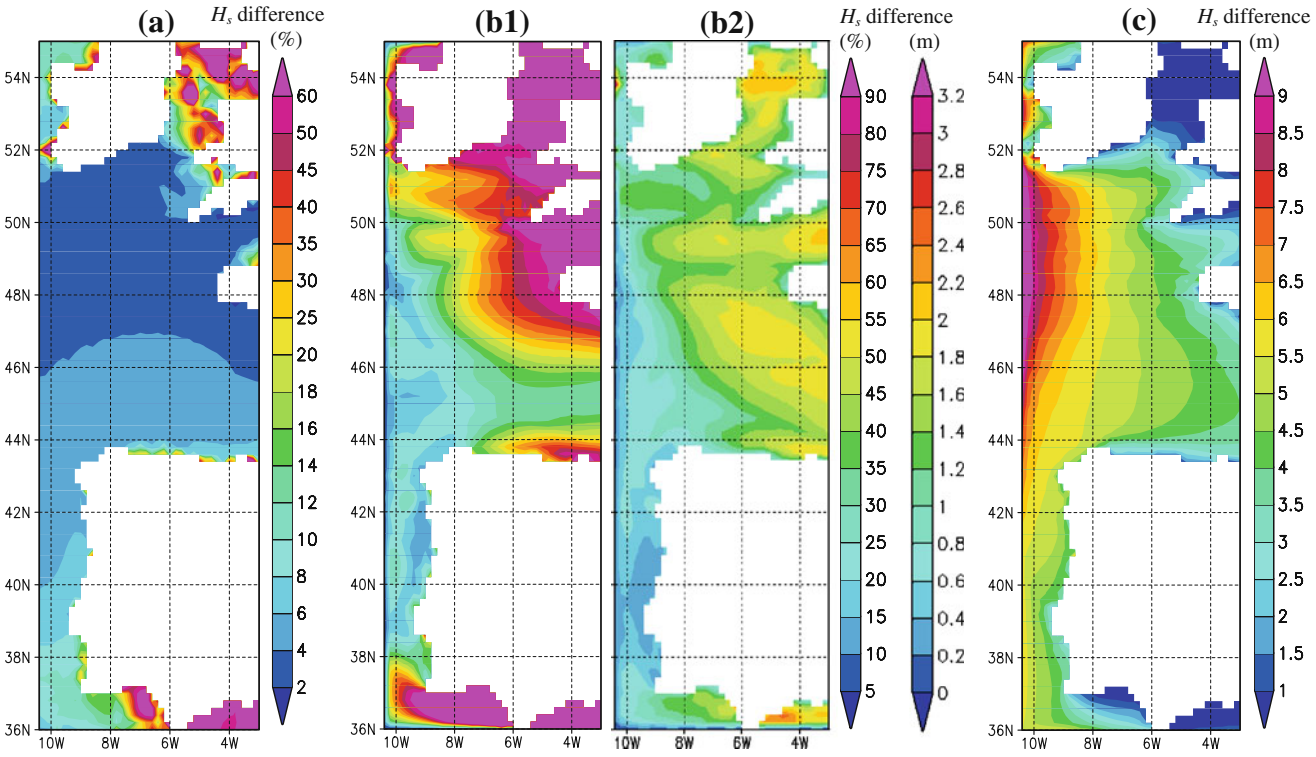

Fig. 2 Maximum differences of hourly H_s over January 1960 between: **a** Benchmark simulation (N1 at 0.2×0.2° resolution) and the set-up of Fig. 1, both forced with ECHAM5 winds, (**b***1*, *2*) benchmark simulation and that when domain N4 is forced by CLM winds (**b***1*, *2* show percentage and absolute H_s differences, respectively) and **c** the nested simulation over N4 and that when N4 is a stand-alone domain without forcing at its boundaries

eastern Atlantic approach west of the North Sea and south of about 52° N. Relatively smaller benefit was obtained at coastal locations north and west of Spain. It should be stressed that this study assumes a benefit from the use of CLM–RCM wind forcing over the N4 domain, as evidenced in the existing literature, without further testing. It should also be noted that different sensitivities of the ECHAM5 GCM winds to the CLM–RCM downscaling are expected in comparison with previous studies. This is because of: the different grid resolution of the RCM winds used in the present study (≈2×resolution of the aforementioned literature); the different GCM–RCM formulation consistency; the absence of data assimilation, which is not relevant for climate change simulations in contrast to hindcast simulations.

The importance of swell propagation can be seen in Fig. 2c. This compares the situation when N4 is forced by CLM–RCM wind fields and boundary wave conditions from the benchmark, with a run when no wave forcing is applied at the N4 boundaries. Wave height differences of up to about 5 m are observed near the coast. Over shelf regions away from the west boundary of the N4 domain, i.e. UK, France and northeast Spain, these should be mainly due to the omission of swell from the latter simulation. Over shelf regions closer to the west boundary of the N4 domain, i.e. northwest Spain down to the Strait of Gibraltar, the reduced fetch imposed by the west boundary of the stand-alone domain could also play an important role in the observed differences as it can prevent the full development of local wind waves. In any case, the results indicate that the commonly limited coverage of RCM experiments is most likely inadequate for obtaining 'reliable' estimates of relative changes in wave climate statistics along the west-European shelf seas. Thus, nesting domains forced by RCM winds within domains forced by GCM winds will mitigate some of these inadequacies. Resorting to RCM climate change experiments over very large areas is very computationally expensive. In addition, there might be little or no benefit from RCM downscaling over Atlantic regions where mesoscale phenomena (e.g. mesocyclones) are rare (e.g. Winterfeldt and Weisse 2009). According to Harold et al. (1999) the centres of mesocyclone activity in the North Atlantic are north of 60° N and to the west of the British Isles.

2.4 Time-slice simulations and statistical analysis

Table 2 shows the wave model runs performed in this study. For each run, the forcing wind field from either the coarse ECHAM5 GCM or the downscaled CLM–RCM is identified against the combinations of nested domains and for each climate change scenario. The number of realisations is also presented, which is dictated by the model-data available for this study. Each run produces a time-slice wave climate in the form of a 40-year three-hourly time series of significant wave height, H_s, mean wave period, T_m and mean wave direction, θ, over all the nested model grids. Three different simulations are performed for the control and climate change scenarios B1 and A1B: (a) coarse ECHAM5 winds force all domains, N1 to N4; (b) same as a, except for regional higher resolution CLM winds force domain N4; and (c) N4, is forced by regional CLM winds alone with no other wave forcing at its boundaries. For scenario A2, only simulation (a) was possible since no CLM A2 experiment is available.

In our analysis, certain statistical measures from the control are compared with the same measures from a scenario for each individual grid point. The statistics are calculated as annual or seasonal (quarterly) quantities. Therefore, for each run there are either 40 values of the wave statistics for a single realisation or 80 values when two realisations are used. These constitute a sample with a spread defined by the interannual variability. The control sample is then compared with a corresponding scenario sample to identify significant differences in their means. In general, the samples are not normally distributed. As a result, the non-parametric Wilcoxon rank-sum hypothesis test (e.g. Freund 1992) which makes no assumptions on the distribution of the samples is selected for the comparison. Although, in theory, a parametric test is more robust, application of a Student's t test revealed that results remained unchanged. The Wilcoxon rank-sum test accepts or rejects the hypothesis that the two samples are the same with a 95% confidence interval, meaning that it allows a 5% probability (maximum) that the test result is false. For clarity, the relative percentage change C_Q in a quantity Q is defined as

$$C_Q = \frac{Q_{\mathrm{Sc}} - Q_{\mathrm{Ctr}}}{Q_{\mathrm{Ctr}}} \times 100 \qquad (1)$$

where the subscripts Sc and Ctr denote the scenario and control value of Q respectively.

Mean H_s values are used to assess relative changes in the overall wave climate. The annual and seasonal 99 percentiles of H_s—a relatively robust statistical measure for the analysis of extremes—are used to investigate relative changes in the extreme waves in the time series. Fields of the results are presented in section 3. A more thorough analysis of the extremes is performed at 4 locations (Fig. 3 and Table 3) within domain N4 (Fig. 1). These include: (1) southwest of UK, north of Cornwall, denoted as 'WH'; (2) northwest of France, west of Brittany, denoted as 'WB'; (3) north of Spain, in the Bay of Biscay, denoted as 'BB'; and (4) offshore from the north of Portugal, denoted as 'PO'. Various methods have been proposed for determining

Table 2 Type of wind forcing for each WW3 domain of Fig. 1 for the various wave climate simulations

Climate change experiments	WW3 nested domain				
	N1	N2	N3	N4	No. of realisations
Control	ECHAM5	ECHAM5	ECHAM5	–	2
	ECHAM5	ECHAM5	ECHAM5	CLM	1
	–	–	–	CLM	1
B1	ECHAM5	ECHAM5	ECHAM5	–	2
'Low emissions'	ECHAM5	ECHAM5	ECHAM5	CLM	1
	–	–	–	CLM	1
A1B	ECHAM5	ECHAM5	ECHAM5	–	2
'Intermediate emissions'	ECHAM5	ECHAM5	ECHAM5	CLM	1
	–	–	–	CLM	1
A2	ECHAM5	ECHAM5	ECHAM5	–	2
'High emissions'					

extreme wave statistics (e.g. Van Heteren and Bruinsma 1981; Muraleedharan et al. 2007; Holthuijsen 2007; Li et al. 2008; Thompson et al. 2009), but here we extract annual maximum values at selected locations to fit a generalized extreme value distribution (GEV) and derive return level plots (RLPs) with confidence intervals for every wave climate. The stationarity of the annual maximum values of H_s, an assumption underlying the GEV fitting, was confirmed at the 95% confidence interval. To get a better insight into how extremes might change in the future we complement the RLPs with quantile-quantile-plots (qq-plots) of the 100 most extreme values from the control against the 100 most extreme values from the scenario. Each extreme value is selected so that it represents an independent event. This is interpreted, as in Debernard et al. (2008), as requiring a spacing of at least 48 h between events.

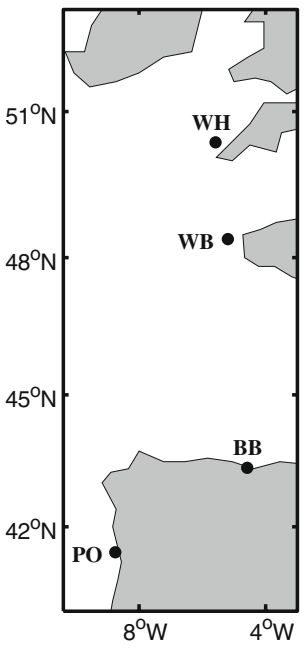

Fig. 3 Locations of extreme analysis

3 Results

3.1 Annual statistics

Figure 4 shows relative changes (Eq. 1) in annual mean (top row) and annual 99 percentile (bottom row) of wind speed, V_H, between the ECHAM5 control and the respective individual scenarios over the N3 domain. In this figure, as well as in the subsequent figures, the areas of statistically significant changes are shown in light grey shading and the relative percentage change in the samples' mean is illustrated by contours. The relative changes in the annual mean wind speed are negative over almost the entire domain, i.e. on average, a less energetic future is projected. No change or very small positive changes (<2%) are mostly found for the higher emissions scenarios A1B and A2 and are confined to the Irish Sea, north and west of Ireland. The reduction in future mean V_H increases along a diagonal from the southwest of UK to the southwest of the N3 domain and becomes more pronounced when moving from

Table 3 Locations of the analysis on extreme wave heights

Location	West longitude	North latitude
WH	5.6°	50.4°
WB	5.2°	48.4°
BB	4.6°	43.4°
PO	8.8°	41.4°

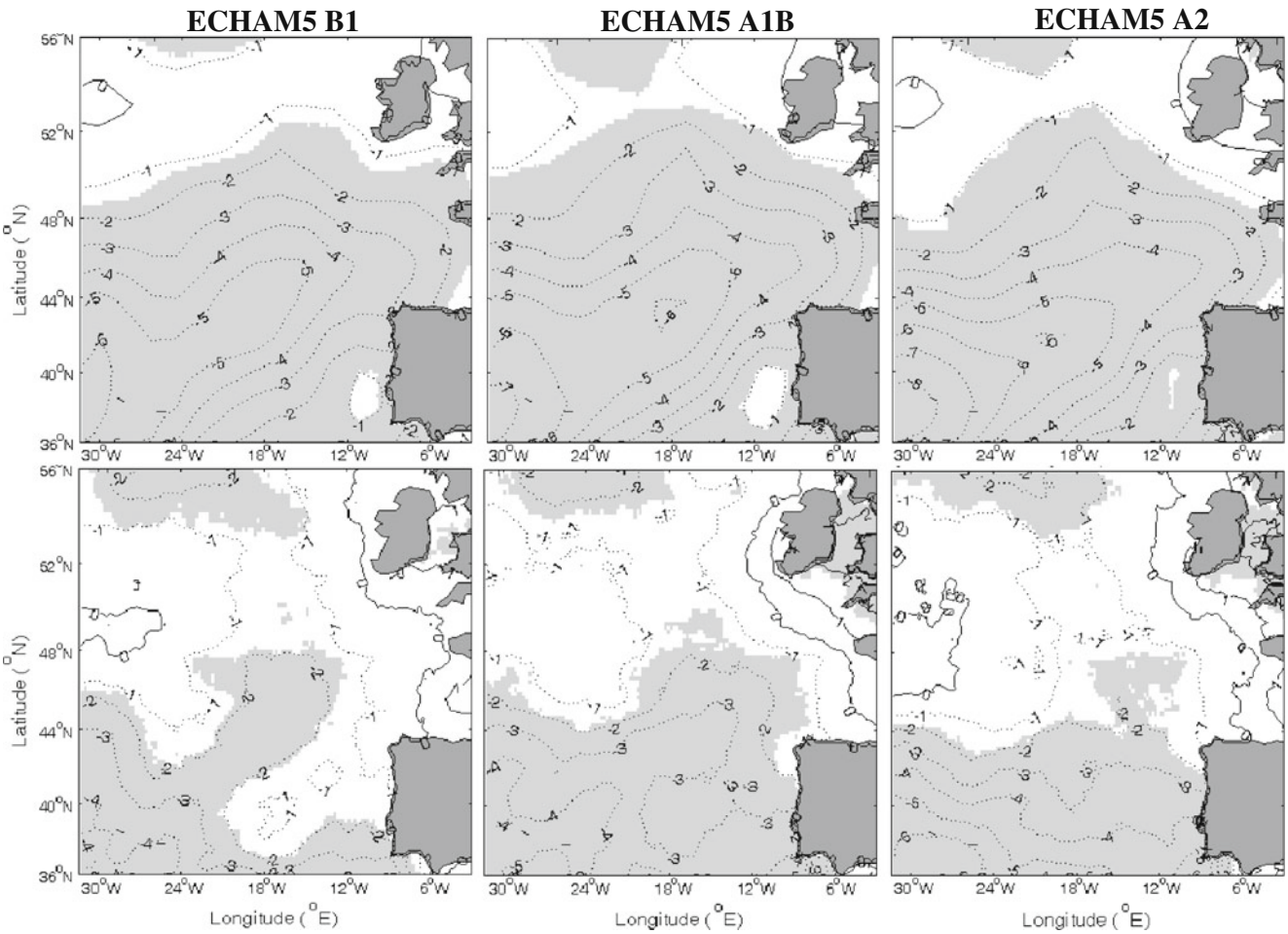

Fig. 4 Relative changes (Eq. 1) in the annual mean (*top*) and annual 99 percentile (*bottom*) of wind speed, V_H. The changes are between the labelled scenarios and the control. Grey-shaded areas denote changes of statistical significance

the lower emissions to the higher emissions scenarios (8% maximum reduction). The changes are statistically significant mostly within the southern two thirds of the domain. In contrast to the annual mean, the annual 99 percentile increases for all scenarios (<3%) along the west-European continental shelf, north of about 44° N. As with the annual mean, it decreases within the rest of the domain. However, this decrease is of a lower percentage—maximum of 6% reduction for the A2 scenario. Changes of statistical significance are less widespread than those of the annual mean. They are mostly found within the southern half of the domain and mainly for the A1B and A2 emissions scenarios.

Figure 5 shows the corresponding relative changes in significant wave height, H_s. Unsurprisingly, the pattern of H_s changes is largely consistent with that of the V_H changes on which it strongly depends. In fact, according to the theory for fully developed seas (WMO 1998), i.e. when wind waves are not limited by fetch, H_s is proportional to V_H^2. Thus, a change in V_H would lead to a larger change in H_s, as is indeed the case in Fig. 5. However, H_s also depends on a number of other parameters, such as wind duration, fetch and the interaction of local wind waves with swell from distant sources. Therefore, discrepancies between the V_H and the H_s changes are to be expected. For example, a future decrease in the annual 99 percentile of H_s is projected within the Bay of Biscay where the annual 99 percentile of V_H increases slightly. This is most probably because future wind directions corresponding to the higher winds in the time series were found to exhibit an anticlockwise shift towards the south compared with the control. Figure 6 provides an example of this observation at the BB location of Fig. 3. As a result, within the Bay of Biscay, extremes in the scenario are more fetch limited than present extremes. In general, as shown in Fig. 7, the future annual mean wind direction shifts clockwise towards the west in most of the southern part of the N3 domain (Fig. 1) and anticlockwise towards the south-southeast in most of the northern part of the domain. The largest shifts are

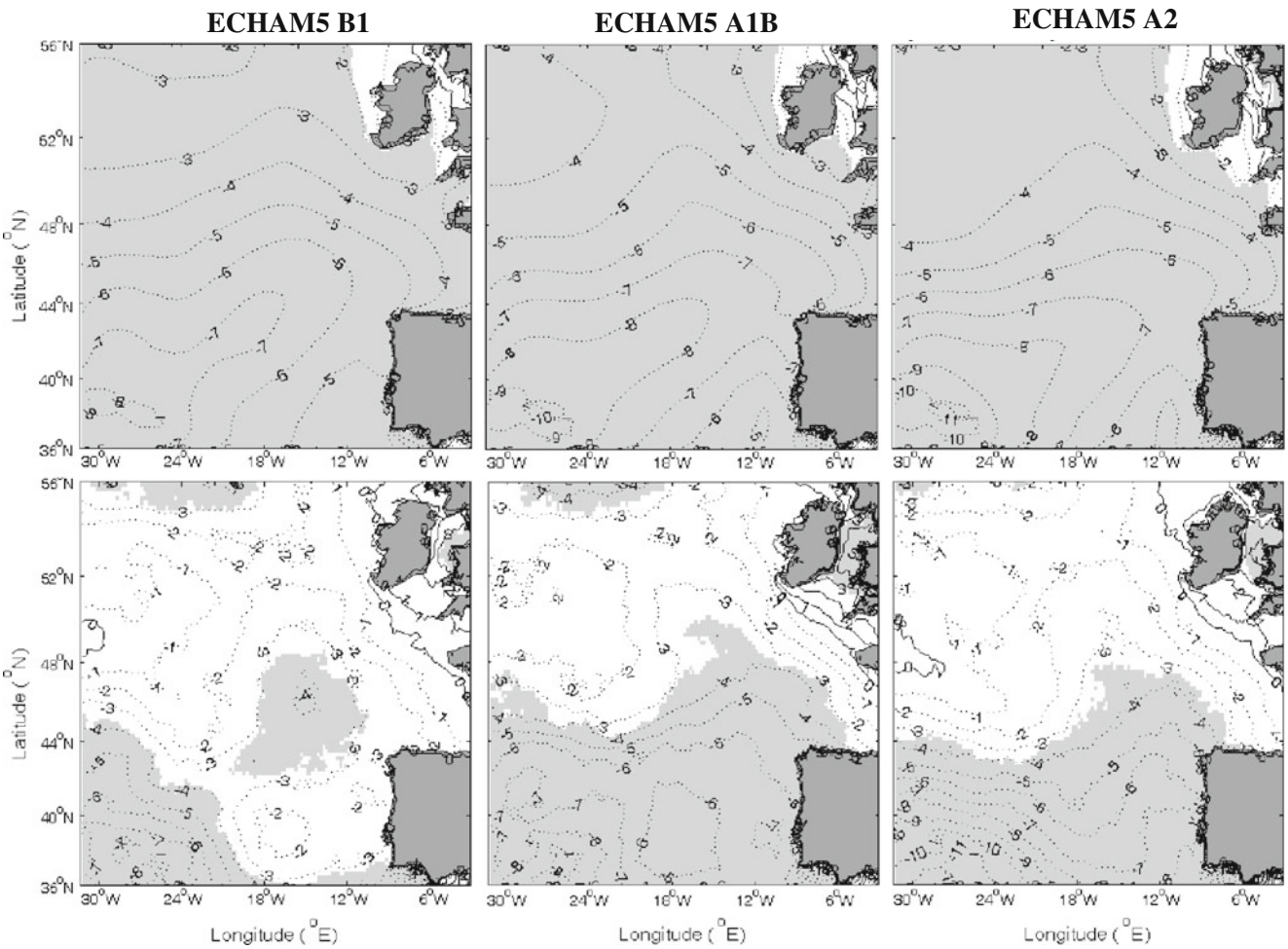

Fig. 5 Same as Fig. 4 but for H_s

observed for the A2 scenario (up to 10° shift clockwise towards the west and 15° anticlockwise towards the south-southeast). Results for scenario A1B are very similar to those of B1. Andrade et al. (2006) (cited in Andrade et al. (2007)), using control and A2 scenario wind fields from a coarse resolution GCM to force a third-generation wave model, have found a clockwise shift (up to about 10°) in future annual mean wave direction over almost the entire domain shown in Fig. 7.

The complex relation between wind characteristics and H_s is also responsible for the different spread of statistically significant changes observed for V_H and H_s. Thus, relative changes in the annual mean H_s are statistically insignificant only in the northeast part of the N3 domain, i.e. in the Irish Sea, west and north of Ireland. Also, compared with V_H, statistically significant changes in the annual 99 percentile of H_s spread eastwards along the northwest Spanish coast for the A1B and A2 scenarios.

Having confirmed that, as might be expected, the relative changes in the wave climates are strongly aligned with those of the wind climates, we now focus on the relative changes of H_s alone and the sensitivity of them on wind input resolution and model coverage. We also focus specifically on domain N4.

3.2 Seasonal statistics

Figure 8 shows relative changes in the seasonal mean (left four plots) and seasonal 99 percentile (right four plots) of H_s between the ECHAM5 control (nested domain N4 forced by ECHAM5 winds) and the corresponding A1B scenario. This figure is contrasted with Fig. 9b, where the relative changes (Eq. 1) between the CLM control (nested domain N4 forced by CLM winds) and the corresponding A1B scenario are shown. Differences between the two sets of results demonstrate the sensitivity to the spatial and temporal resolution of the forcing. In general, we see that the pattern of these changes is very similar in the two cases; as is the pattern of statistical significance. This is true for both the mean and the 99 percentile of H_s. Nevertheless, differences do exist. Differences in the sign of the relative changes are observed during spring and summer. Thus, in

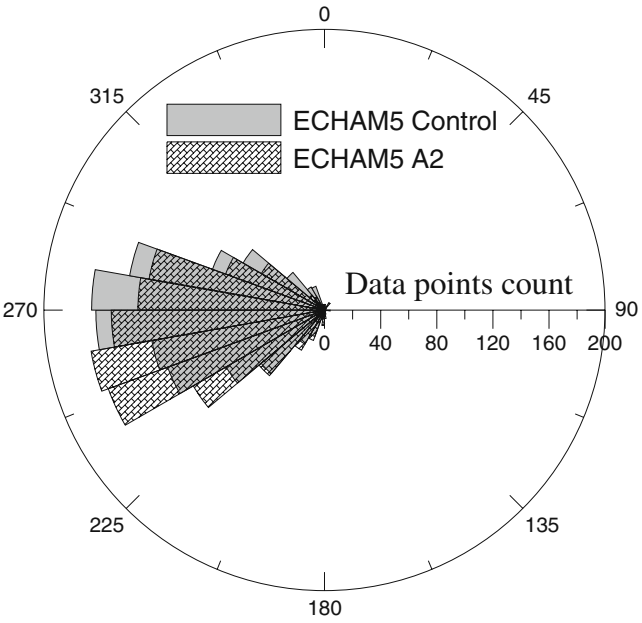

Fig. 6 Control vs. A2 scenario wind directions of extreme winds at the BB location of Fig. 3

summer, a region of positive changes in mean and 99 percentile of H_s found offshore from the north of Portugal for the CLM A1B scenario is displaced southwards for the ECHAM5 A1B scenario. This, in turn, alters the area over which the changes are significant. In addition, in spring, positive changes in the Irish Sea found in the 99 percentile of H_s for the ECHAM5 A1B scenario coincide with negative changes in the CLM A1B scenario. Not surprisingly, the differences between CLM and ECHAM5 results are generally the greatest (2–5%) at the Irish Sea. This is because wind characteristics in this region are expected to vary within finer scales than those resolved by ECHAM5 due to the proximity of the surrounding land. Furthermore, differences are somewhat greater for the 99 percentile of H_s. This was also to be expected (e.g. Kaas and Andersen 2000; Winterfeldt and Weisse 2009) since extremes vary within finer temporal and spatial scales than mean climate. Away from the regions of higher discrepancies, differences are typically 1–2%. The pattern and magnitude of differences between the control and B1 scenario (not shown) are similar to those shown above for the A1B scenario.

As a result, it is reasonable to compare the results obtained for the CLM B1 and A1B scenarios with those obtained for the ECHAM5 A2 scenario (no CLM A2 scenario is available), keeping in mind the discrepancies that are likely to exist over certain regions and seasons, as shown in Fig. 9. In winter, the mean and 99 percentile of H_s will increase offshore from France, UK and Ireland for all emissions scenarios. The relative increase is more pronounced for scenario CLM A1B. It begins along the eastern boundary of the domain at about 45° N (offshore from Bordeaux, France) and is progressively larger towards the north. For mean H_s, the increase is 3% west of Brittany, 4–8% south-southwest of UK, up to about 10% in the Irish Sea and statistically significant around UK. For extreme H_s, the increase is greater. It ranges from 8% west of Brittany to 11% to the southwest of the UK. The area over which changes are statistically significant is also greater, extending further to the west and south, including now the waters around Brittany. The increase is smaller (up to 7%) for the ECHAM5 A2 scenario. Also, in contrast to CLM A1B, the increase of the future 99 percentile of H_s for this scenario (up to 5%) is less than that of the mean. Increases are now observed within the entire Bay of Biscay, being around 1–3% from the north of Spain to the west of France. These changes are significant only for the mean H_s and over roughly the same area as for the CLM A1B scenario. For scenario CLM B1, the winter increase in H_s is even smaller and insignificant.

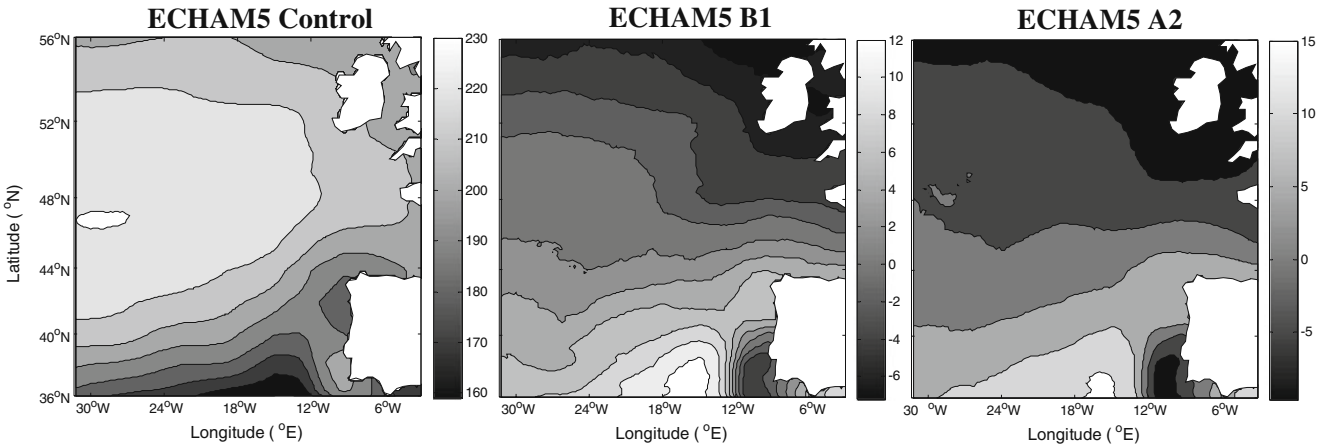

Fig. 7 Control annual mean wind direction (*left*) and differences between control and scenarios

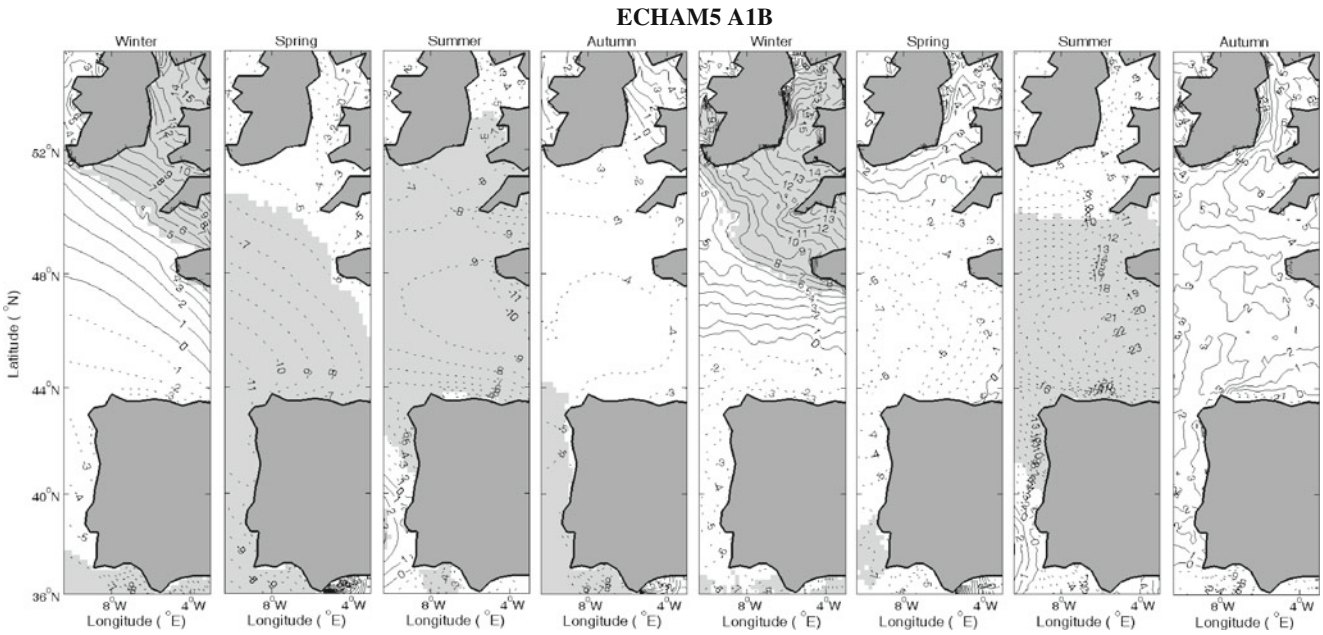

Fig. 8 Relative changes (Eq. 1) in the seasonal mean (*left* four plots) and seasonal 99 percentile (*right* four plots) of H_s. The changes are between the labelled scenario and the corresponding control. Grey-shaded areas denote changes of statistical significance

Shifting our attention to the southern part of the N4 domain, we see that this is characterised by a future wave climate of lower H_s (up to 5% reduction). This decrease, common amongst scenarios and statistical measures, is generally not significant. Significant changes are found below 40° N for the B1 and A2 scenarios. These reach up to ≈9% west of the Strait of Gibraltar. However, there is less confidence in the results obtained over those regions lying close to the north and south boundaries of the N4 domain, as may be affected by the nesting procedure described in section 2.2 (see Fig. 2a).

In spring, summer and autumn, results are very different compared with winter. Over these seasons, the general image is one of lower future H_s values. In summer, mean H_s significantly decreases, 8–11%, over most of the domain north from the north coast of Spain. The decrease is smaller along the Spanish coast, 4–8%, but still significant. The changes are fairly consistent amongst scenarios. For the 99 percentile of H_s, a greater future decrease is obtained. Its maximum is observed within the Bay of Biscay and is 24%, 20% and 17% for the CLM A1B, ECHAM5 A2 and CLM B1 scenarios respectively. Only north of about 51° N, future changes in the 99 percentile of H_s are somewhat smaller compared with mean H_s changes. In turn, the extent of the northern domain characterised by statistically significant changes is squeezed, particularly for the CLM B1 scenario. An area of insignificant small positive changes is present west of Portugal (south of about 42°N) for both statistical measures. In spring, mean future H_s decreases everywhere in the domain of interest. Compared to summer, the decrease is smaller in the Bay of Biscay and to the north, but larger from the northwest of Spain to the south. It is significant over at least the lower two thirds of the domain examined but not for the CLM B1 scenario for which smaller, largely insignificant changes occur. For the 99 percentile of H_s, changes are considerably smaller. They are significant only for the ECHAM5 A2 scenario, from the north-northwest of Spain to the south of the domain. In autumn, decreases in mean future H_s are smaller than in spring and summer. They are mainly significant for the ECHAM5 A2 scenario, south of the English Channel. For the 99 percentile of H_s, a greater future decrease is projected for this scenario. This is in contrast to scenarios CLM A1B and B1 which show small increases that are not statistically significant.

This study uses a sole GCM–RCM combination to produce its results—an approach that was considered more suitable for studying the sensitivity of the results to the domain extent (related to swell representation) and the spatial and temporal resolution of the forcing. In consequence, uncertainties in simulated climatic scenarios introduced by the use of different GCMs and RCMs are not treated. Qualitative results obtained from the use of different RCMs have been found to be mostly consistent. However, it is generally accepted that the greatest uncertainty in climate scenarios is due to the use of different driving GCMs (e.g. Räisänen et al. 2003; Pryor et al. 2005). Nevertheless, the results of this study are in good agreement with the multi-model results (different driving GCMs) of Debernard et al. (2008). In

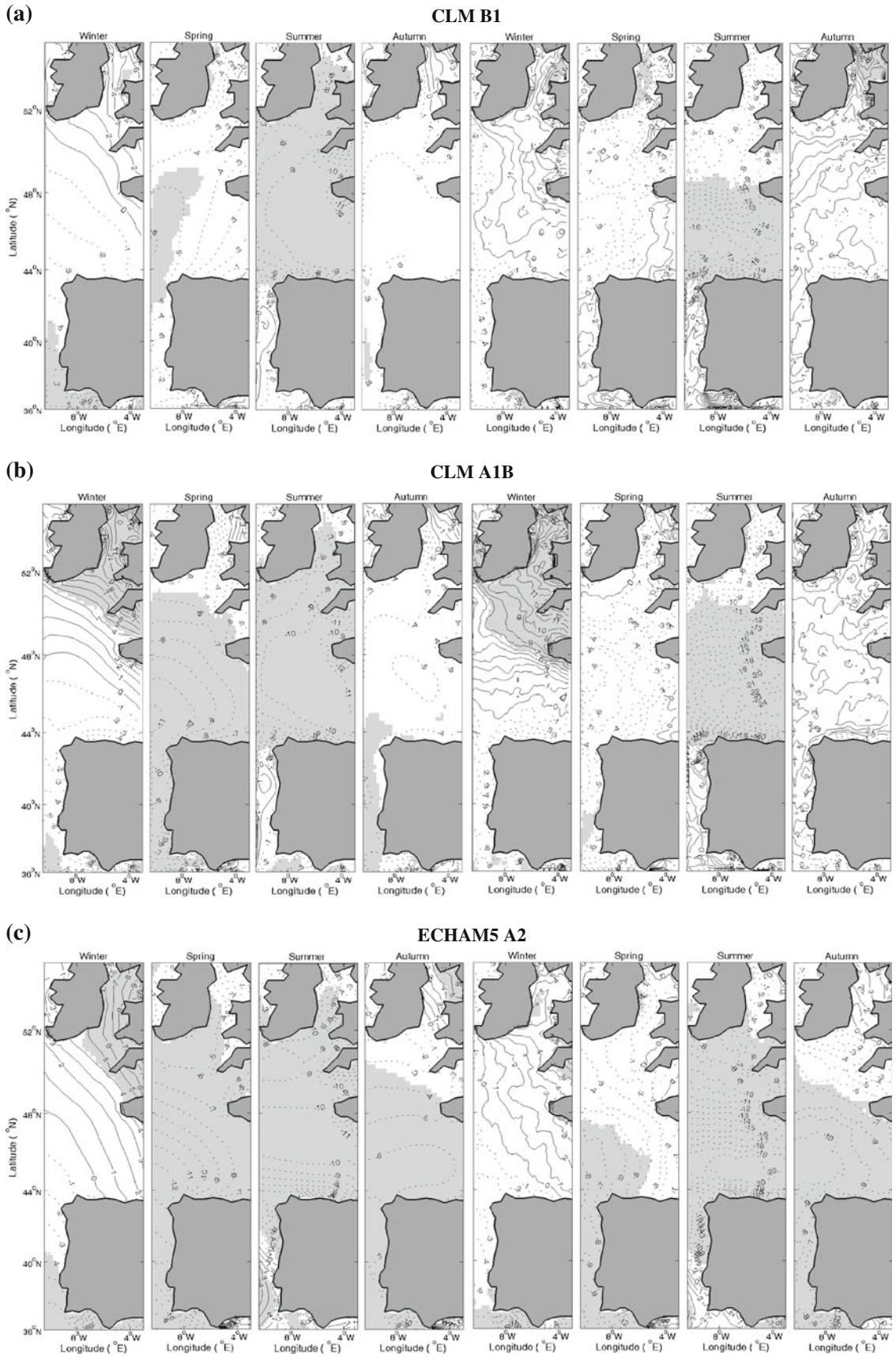

Fig. 9 Same as Fig. 8

their multi-model approach they included downscaled versions of the control, B2—the scenario of higher emissions than B1 after about 2070 but lower than A1B—and A1B scenarios over the time-slices 1961–1990 and 2071–2100. Their downscaling extended beyond the west limit of typical RCM simulations to about 30° W whilst the southern boundary was set at about 40° N. They projected an increase in future winter mean H_s of similar magnitude and significance to that displayed by the A1B scenario in Fig. 9b. Similarly, they found a summer decrease close to the one shown for the same scenario. The pattern of changes in the yearly 99 percentile of H_s they projected is also consistent with the one found in this study for the CLM A1B scenario (not shown, but very similar to the winter pattern). Nevertheless, the study of Debernard et al. (2008) predicts larger relative increases and smaller decreases of extremes in the future. Wang et al. (2004) found different trends with very little regional consistency in the changes of mean H_s between different scenarios. Around UK, north of 48°N, Lowe et al. (2009) also reported quite different results. Analysing the same time-slices as in Debernard and Røed and the A1B emissions scenario, they found that mean future H_s will either stay unchanged or decrease in all seasons within the N4 domain. They projected future increases only in summer, offshore from the north coast of France. Regarding extreme values, significant increases were found in the winter maxima of H_s south and west of UK. This result is in agreement with our study and others (e.g. Beniston et al. 2007; Räisänen et al. 2004). The difference of the UKCIP09 and this study's results on mean H_s changes is likely to be related to the different GCM–RCM combination used. The different wave model, wave model set-up and time-slice periods are expected to have also contributed to the divergence of the studies' outputs. UKCIP09 also presented two additional outcomes corresponding to different climate model climate sensitivities (i.e. perturbed model physics). The discrepancies between outcomes of different climate sensitivities were shown to be substantial.

We now examine how the sole use of typical RCM experiments rather than GCM—RCM combinations might influence the results presented in Fig. 9. Figure 10 shows the results for the CLM A1B scenario but when domain N4 in Fig. 1 is a stand-alone domain. There are substantial differences between the results of Fig. 9b and those of Fig. 10. These differences concern the strength of the relative changes, the area over which the changes are statistically significant, and occasionally the direction of change. A general observation is that future tendencies in mean H_s are largely the same in the two figures but larger relative changes occur in the case of the stand-alone N4 domain in Fig. 10 (except in spring over the northern part of the domain). Differences between the two cases are greater in summer, when the swell component is expected to be most important. For example, differences of up to 6% are found southwest of UK for this season. They increase to the south, reaching about 10% offshore from the northwest of Spain. In winter, the range of the respective differences is 2–5%. Statistically significant changes are found over a much larger area in autumn in Fig. 10 than in Fig. 9b. This is also the case in winter in the southern domain. In general, differences between the two cases are greater along exposed coastal regions which lie close to the western boundary of the domain, i.e. northwest of Spain and Portugal. This is reasonable since this boundary not only prevents the propagation of swell into the region but also, as already mentioned with respect to Fig. 2c, poses an obstacle to the sufficient development of local wind waves. The nesting procedures employed in this study are believed to greatly improve the results over such regions. Yet, considerable discrepancies are also found away from the western boundary. They clearly indicate the significant influence of swell on the results and the inadequacy of typical RCM coverage to account for it.

Comparing the seasonal changes in the 99 percentile of H_s in Figs. 8b and 9, we note that relative changes have now a different sign over some regions. For example, in autumn, a reversal of the direction of change from positive to negative changes is seen over a large part of the domain. However, the differences are smaller for the 99 percentile than for the mean H_s. This is particularly evident in summer, where differences between the two figures do not exceed 2% from the north of Spain to the north of the domain. Moreover, the pattern of statistical significance in the seasonal 99 percentile of H_s is very similar between the two cases. This is not a surprising outcome since local wind waves, associated with Fig. 10, are mainly responsible for the higher waves in a time series.

We also examined the changes between control and scenario in absolute terms (not shown) for the nested and the stand-alone N4 domain. We found that nearly everywhere and in all seasons with the exception of spring, the mean H_s of wind waves computed with the stand-alone domain, decreases more in the future relative to the control conditions than the corresponding change in the total spectrum. The same absolute future increases are observed in winter over the northern half of the domain. The implication of this is that the pattern of the relative changes in Fig. 9 is dominated by waves generated by local winds. Especially in winter, future changes in the mean H_s of locally generated waves are mainly responsible for the increases observed in Fig. 9 over the northern N4 domain. Over the rest of the domain, in contrast to the average behaviour of locally generated waves, the swell component should be growing in the future so as to shift the differences

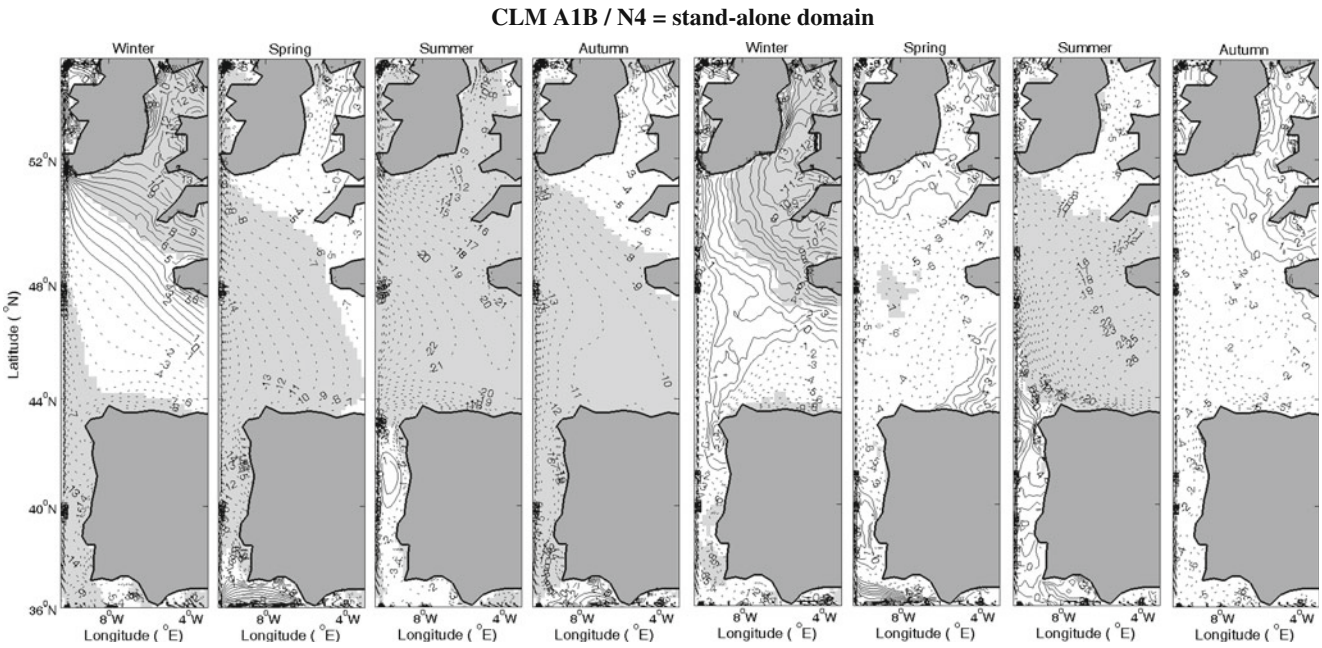

Fig. 10 Same as Fig. 8

between scenario and control towards those found for the nested run. In spring, the situation is different. During this season, the mean H_s of the total wave spectrum decreases more in scenario conditions than does the mean H_s of the local wind waves alone. This suggests that waves propagating into the N4 domain across its west boundary also decrease in height in the future. A similar analysis was carried out for the 99 percentile of H_s, from which a growing swell component is inferred everywhere in the domain in summer, winter and spring.

3.3 Extreme analysis at selected locations

It is particularly important to understand how extremes might be affected by global warming as it is these conditions that affect the performance or threaten the integrity of offshore engineering structures or nearshore sea defences, often posing a risk to human assets. Therefore, in this section, we examine in more detail the behaviour of these events at the four locations shown in Fig. 3 and for the different wave climates considered in this study. Figure 11 (left) shows RLPs with confidence intervals for the CLM control and the CLM future wave climate scenarios at the four selected locations. The two bottom figures include results from the stand-alone N4 domain wave model runs (red lines). Figure 11 (right) shows qq-plots of H_s for the 100 largest events from the CLM control plotted against the 100 largest events from the CLM scenario. Again, the two bottom figures include output that corresponds to the stand-alone N4 domain simulations. Figure 12 is the same as Fig. 11 but, in this case, the results from the CLM forced simulations are compared with those from the ECHAM5 forced simulations (red lines) at location BB.

Figure 11 (right) shows that the future extremes, irrespective of scenario, are larger than those at present at locations WH and WB, which are situated within the northern part of the N4 nested domain. The CLM A1B scenario corresponding to medium–high emissions is more energetic than the CLM B1 scenario of low emissions. At the WH location, the highest events in the time series (≈10 events) diverge considerably between the two scenarios. For the CLM A1B scenario, the top extremes show a bigger increase (10–17%) relative to the control compared with the rest of the events (<10% increase). For the CLM B1 scenario, these extremes gradually converge as the severity of the event increases to the respective extremes of the control and ultimately become lower (<±5% relative differences). At the WB location, this behaviour is evident for both scenarios but is still more pronounced for B1. At this location, the largest relative differences are ±10% and relate to the 20 largest events in the time series. The appearance of the qq-plots is different at locations BB and PO, situated within the southern part of the domain. At these locations, the deviation of the scenario extremes from the respective control extremes is, in general, in opposite directions for the two different scenarios. The CLM B1 extremes are higher in the future relative to the present contrary to the CLM A1B extremes which are lower. This is fairly consistent for all events apart from the most severe (≈10 events), which, in their majority, are higher in the future for both scenarios but show a more variable pattern.

In any case, the differences observed at these locations do not exceed 5%.

At all four locations, the results closely mirror the results for the relative changes in annual 99 percentile of H_s between control and scenario. These are not shown, but are well represented by the winter 99 percentile changes shown in Fig. 9. Some disagreement exists for the CLM B1 scenario at locations BB and PO. Figure 11 (right) indicates a general small increase in extreme wave heights relative to the control whilst Fig. 9a shows a small relative decrease (PO) or no change (BB) in the mean winter 99 percentile of H_s. By extending the qq-plots so as to incorporate data points related to lower H_s values, we found that the CLM B1 H_s decrease relative to the control for H_s<5 m at location BB and H_s<6 m at location PO. The annual 99 percentiles of H_s at BB and PO are mainly below 5 m and 6 m respectively, leading to the aforementioned discrepancy between Figs. 10 and 8a. In any case, differences in extreme H_s between control and scenario do not appear to be significant at these southern locations. This is evident in Fig. 9 but also from the RLPs in Fig. 11 (left). Specifically, the control wave climate and the two scenario wave climates have very similar RLPs with largely overlapping confidence intervals. In the qq-plots of Fig. 11, the highest departures from the extremes of the control were found at locations WH and WB from the respective extremes of scenario CLM A1B. CLM A1B is the only scenario for which statistically significant increases were found in the winter 99 percentile of H_s over the northern N4 domain. Nevertheless, the RLPs associated with these northern locations (Fig. 11 left) indicate that no significant deviations exist in the return periods of the highest waves in the different time series. However, at WH, the overlapping area of the RLP confidence intervals of CLM control and A1B scenario is substantially less than that shown for the other locations. In particular, at return levels in the range of 4–10 years, the upper confidence interval limit of the control is very close to or slightly overlaps the lower confidence interval limit of the A1B scenario. The CLM A1B H_s with return period within this range are about 1.5 m higher than the respective control H_s.

The bottom four graphs of Fig. 11 reveal the impact on extreme values when no wave forcing was applied at the boundaries of the N4 domain. Figure 11, bottom left, shows very big differences in the return period plots between the two cases. The smallest of these differences are found at location BB where the RLP confidence intervals of the two cases overlap for the CLM control and the CLM A1B scenario and for return periods greater than 20 years. The largest differences are found at location PO where discrepancies reach 4.5 m and no overlap exists. At locations WH and WB (results from stand-alone N4 not shown), an intermediate situation was observed. Specifically, at WB, the overlap is similar to that shown for location BB but it occurs at greater return periods (≥40 years). At WH, the overlap occurs only for scenario CLM A1B and for return periods greater than 50 years. Reasonably, the further away from the west boundary of the N4 domain, the smaller the discrepancies between the two cases examined. Yet, they are still substantial. In Fig. 11, bottom right, the relevant qq-plots clearly show that the extremes resulting from the N4 stand-alone runs have considerably smaller H_s than those resulting from the nested N4 runs, particularly at location PO.

Fig. 11 *Left*, return period plot with confidence intervals (ci) for the CLM control and the CLM scenarios at the four locations indicated in Fig. 3. The *red lines* correspond to the results for the stand-alone N4 domain; r*ight*, qq-plots of H_s for the 100 largest events from the CLM control plotted against the 100 largest events from the CLM scenario

At BB, Fig. 12 shows that the discrepancies between results related to the CLM wave climates and those related to the ECHAM5 wave climates are not trivial. However, they are considerably less than those found between nested and stand-alone N4 domain runs. In Fig. 12, left, the differences in RLPs corresponding to the two cases (≤1 m) are found to be significant only for the B1 emissions scenario and for return periods in the range of 2–20 years. No significant differences are found at the rest of the locations. At location WH (not shown), the magnitudes of discrepancies are similar to those at BB whilst much smaller discrepancies are observed at WB and PO (not shown). As mentioned in section 3.2, this has to do with the complexity of the topography around the selected locations, which is not well represented in the coarse resolution ECHAM5 wind input time series. Thus, WH and BB are associated with a more complex surrounding topography compared with WB and PO which are more exposed to the Atlantic.

4 Discussion and conclusions

In this paper, potential future changes in the wave climate of the west-European shelf seas from 37° to 52° N have been assessed, using the WW3 wave generation model, forced by surface wind fields. In particular, the WW3 model was set-up to include four one-way nested meshes, which were driven by wind field time series at three-hourly intervals spanning two 40-year time-slices, the control period 1961–2100 and the future period 2061–2100. Three IPCC greenhouse gas emissions scenarios were considered: B1, A1B and A2. Field relative changes between generated control and scenario wave climates were estimated through statistical analysis.

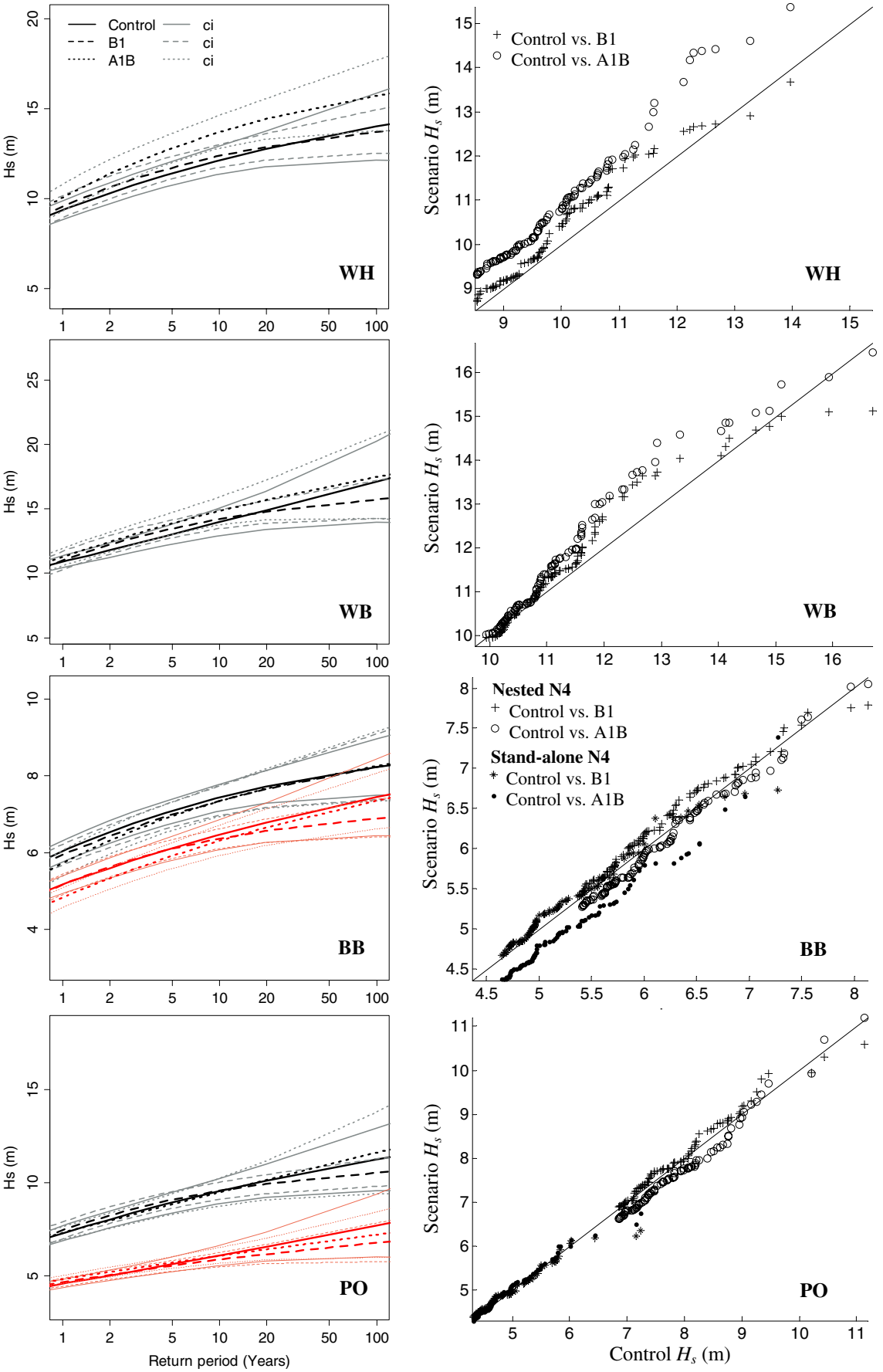
Control
B1
A1B
ci
ci
ci
Hs (m)
WH
WB
BB
PO
Return period (Years)
Control vs. B1
Control vs. A1B
Scenario H_s (m)
Nested N4
Stand-alone N4
Control H_s (m)

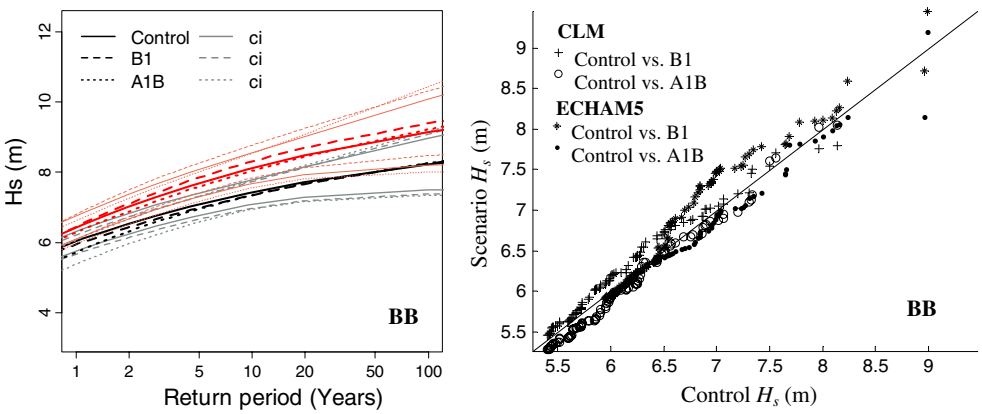

Fig. 12 Same as Fig. 10 but the *red lines* now correspond to the ECHAM5 control and scenario return period plots

At a broad level, this work complements previous work on the potential future changes in the wave climate of the Northeast Atlantic by introducing different climate change scenarios (i.e. different models and/or emissions scenarios) in the analysis. But most importantly, this work shifts the focus of the investigation from the northern seas to the continental shelf of the west Europe from the Irish Sea down to the Strait of Gibraltar. Unlike the North and Baltic Seas, swell is extremely important over this highly exposed domain. Therefore, for the sound investigation of the relative changes between control and scenario wave climates over this region, it is important to investigate changes in the swell component of the wave spectrum. To properly account for this component, wave generation and propagation over the greater part of the North Atlantic Ocean should be considered. Coarse resolution GCM wind fields may be used to force such a broad domain. However, these models are not ideal for assessing regions characterised by wind fields whose changes take place over finer scales than those resolved by the models. For example, they are expected to perform poorly over regions of complex coastal topography. To overcome this, RCMs of considerably finer resolution may be used instead. However, these models are very computationally demanding, often prohibitively so for long-term predictions, and their application over large domains may be constrained. Moreover, in terms of output quality, they may provide no advantage compared with GCMs, over oceanic regions characterised predominantly by large-scale processes. Besides, publicly available RCM climate change experiments have boundaries that typically lie not very far away from the land. Consequently, they are more appropriate for investigations of potential future changes in locally generated waves rather than in the total spectrum of surface waves. Here, we have used publicly available combinations of GCM–RCM experiments, thereby allowing swell propagating into the west-European shelf seas to be included. At the same time, RCM forcing within the inner WW3 nested domain ensures that fine scale wind changes along the west-European coast are well represented.

Many earlier studies have focused on the northwest-European shelf and the North Sea, but paid little attention to the southwest-European shelf. Few have actually reported some changes over this domain, north of the Portuguese Berlengas islands at about 39.5°N. These studies performed RCM experiments beyond the typical west boundary of ≈11°W (<30°W west of Portugal). Nevertheless, swell arriving at the west-European coast if often generated outside the domain considered in these studies. Also, the approach of these studies is demanding as they require access to RCMs and RCM simulations in addition to wave model simulations, and large computational resources. In contrast, this work accounts for all swell by using the forcing from readily available model-based climate change experiments. In addition, the present study demonstrated the sensitivity of the computed changes to the removal of the RCM forcing, i.e. to the sole use of GCM forcing throughout the domain. Also, it examined the sensitivity of the computed relative changes to the removal of the GCM forced meshes, i.e. to the sole use of RCM wind output. Some conclusions on the relative changes in swell as opposed to those in local wind-waves could be drawn this way. The sensitivity of RLPs and qq-plots of extreme values to the above variations was also investigated. The results of the present study can now be summarised.

From a preliminary analysis using GCM forcing, we found that annual field changes in mean future significant wave height, H_s, relative to the present mean (Eq. 1), largely followed the respective changes in mean wind speed, V_H. As anticipated, changes in the former variable were amplified in comparison to those in the latter variable. Also, they were statistically significant over a larger domain. In general, discrepancies in the regional extent over which changes were found to be statistically significant were attributed to the complex dependence of H_s on wind duration and fetch length as well as wind speed. This analysis showed results over a greater area of the Atlantic Ocean than that covered by the RCM experiments. It also

confirmed that H_s changes followed V_H changes, as expected. This is important for establishing the sound application of the wave model since no validation of the control wave time-series was performed. Following Debernard et al. (2008), the underlying assumption is that the estimated relative changes between control and scenario wave climates give a representative measure of the changes due to a warmer climate, irrespective of the level of agreement between reanalysis or observed wave climate statistics and those of the control simulation.

From the combined GCM–RCM seasonal analysis, we have seen that the pattern of the relative changes between control and scenario (Eq. 1) is generally consistent amongst scenarios for all seasons and statistical measures. However, the uncertainty in climate scenarios associated with the use of different GCMs and RCMs was not considered in this study. The main characteristics of the observed pattern are: (1) future increase in mean and extreme H_s in the northern domain in winter; (2) future decrease in mean H_s in spring, summer and autumn over almost the entire domain and in winter over the southern domain; and (3) future decrease in extreme H_s as in (2) but in autumn (insignificant but widespread increase for scenarios A1B and B1). The largest changes were found in summer and are mostly statistically significant. In general, the higher emissions scenarios A1B and A2 gave larger changes than the low-emissions scenario B1. Accordingly, changes of statistical significance covered a larger domain in the former cases. The results of this analysis, especially those corresponding to the A1B emissions scenario, were found to be in good agreement with the multi-model results of Debernard et al. (2008). Also, the projected future increase in the winter 99 percentile of H_s, significant for scenario A1B, was found in the majority of previous studies. Nevertheless, at the four locations selected for further extreme analysis, no significant differences between control and scenario were found in the RLPs. On the other hand, the qq-plots of the extremes displayed results that nicely conformed to the results on the field relative changes discussed above.

The sensitivity of the combined GCM–RCM results to the removal of the RCM forcing revealed that in exposed regions of the west-European continental shelf, future changes in mean and extreme H_s relative to the present and the significance of these changes can be reasonably assessed using only the GCM scenarios. This is not the case in less exposed regions, such as the Irish Sea, where discrepancies between the two cases increased. This agrees, at least conceptually with hindcast studies which found that RCM downscaling of global winds significantly improved simulated wind quality only over regions of complex coastline and high topographic gradients. In summer, a region of positive changes found offshore from north of Portugal in the combined GCM–RCM analysis was observed displaced southwards in the GCM analysis. In general, the observed discrepancies were somewhat higher for the 99 percentile of H_s. However, significant differences in the location specific RLPs of the two cases were found only for emissions scenario B1 in the Bay of Biscay.

However, the sensitivity of the combined GCM–RCM results to the removal of the GCM forcing and using only the inner RCM domain was found to be notable. Substantial discrepancies between the two cases were found over the whole domain indicating the important contribution of changes in the swell component on the combined GCM–RCM results. The largest discrepancies concerned mean H_s changes, especially in summer when the swell component is expected to be most important. Discrepancies in the changes of the seasonal 99 percentile of H_s were generally smaller, since this is typically dominated by local wind waves. Nevertheless, the RLPs obtained at the four selected locations were markedly different between the two cases. This difference was statistically significant for moderate extremes; the difference for the largest return periods not being statistically significant. The qq-plots of the site specific extreme analysis clearly indicated that the combined GCM–RCM analysis produces considerably higher extremes than the stand-alone RCM analysis. The differences between these two cases were far more dramatic than those between control and scenarios.

The direction of future changes in the swell waves as well as the sea waves individually was inferred from the above sensitivity analysis. The results suggest: (1) the pattern of the relative changes in the combined GCM–RCM analysis is dominated by waves generated by local winds, especially in winter over regions where future increase in H_s is projected; (2) wherever the height of future seas was found to decrease in average swell increased, except for spring; (3) in spring, both swell and seas decrease in average height; and (4) for the 99 percentile of H_s, a growing swell component was inferred everywhere in the domain in summer, winter and spring.

In conclusion, this study provides a contribution to the exploration and understanding of potential future changes in the wave climate of the west-European shelf seas, including regions that have barely been investigated. It further improves the understanding of the kind of discrepancies one would expect over this domain from the use of climate models of different resolution and coverage. Specifically, it suggests that forcing from GCM–RCM combinations is the preferable option for the region of interest, especially for the exploration of relative changes in extremes between control and scenario. If this is not possible, GCM forcing can still give good results for both mean and extreme H_s relative changes over regions that are highly exposed to the Atlantic Ocean. In contrast, RCM forcing alone is shown

to be insufficient for exploring wave climate changes over the western European waters. Only changes in the most extreme extremes due to local intense wind storms may be sufficiently accounted for by such an application.

Acknowledgements The climate change experiments used in this work are supplied from the Max Planck Institute for Meteorology and are retrieved from the WDCC/CERA database (WDCC 2009). The authors acknowledge the support of UK South West Regional Development Agency (SWRDA) through grant no. SWR01011. We would also like to thank Dr. Julian Stander (School of Mathematics and Statistics, University of Plymouth) for his valuable advice on the statistical analysis of this work.

References

Andrade C, Pires H, Silva P, Taborda R, Freitas MC (2006). Zonas costeiras. In: Santos FD, Miranda P (eds.). Altera ões climáticas em Portugal. Cenários, impactos e medidas de adapta ão. Lisboa, Portugal, Gradiva. pp. 159–208

Andrade C, Pires HO, Taborda R, Freitas MC (2007) Projecting future changes in wave climate and coastal response in Portugal by the end of the 21st century. J Coast Res 50:263–257

Beniston M, Stephenson DB, Christensen OB, Ferro CAT, Frei C, Goyette S, Halsnaes K, Holt T, Jylha K, Koffi B, Palutikof J, Scholl R, Semmler T, Woth K (2007) Future extreme events in European climate: an exploration of regional climate model projections. Clim Change 81(Supplement 1):71–95

Bouws E, Jannink D, Komen G (1997) The increasing wave height in the North Atlantic Ocean. Bull Am Meteorol Soc 77(10):2275–2277

Caires S, Swail VR, Wang XL (2006) Projection and analysis of extreme wave climate. J Climate 19(21):5581–5605

Cardone V, Jensen R, Resio D, Swail V, Cox A (1996) Evaluation of contemporary ocean wave models in rare extreme events: the "Halloween storm" of October 1991 and the "Storm of the century" of March 1993". J Atmos Oceanic Technol 13:198–230

Castro CL, Pielke RA Sr, Leoncini G (2005) Dynamical downscaling: assessment of value retained and added using the Regional Atmospheric Modelling System (RAMS). J Geophys Res 110: D05108. doi:10.1029/2004JD004721

Chawla A, Tolman HL (2007) Automated grid generation for WAVEWATCH III. NOAA/NWS/NCEP/OMB, Technical Note 254. p 71

Debernard J, Røed LP (2008) Future wind, wave and storm surge climate in the Northern Seas: a revisit. Tellus A 60(3):427–438

Debernard J, Sætra Ø, Røed LP (2002) Future wind, wave and storm surge climate in the northern North Atlantic. Climate Res 23:39–49

Feser F (2006) Enhanced detectability of added value in limited-area model results separated into different spatial scales. Mon Weather Rev 134:2180–2190

Fowler HJ, Blenkinsop S, Tebaldi C (2007) Linking climate change modelling to impacts studies: recent advances in downscaling techniques for hydrological modelling. Int J Climatol 27:1547–1578

Freund JE (1992) Mathematical statistics. Prentice-Hall, New Jersey, 576

Grabemann I, Weisse R (2008) Climate change impact on extreme wave conditions in the North Sea: an ensemble study. Ocean Dyn 58(3–4):199–212

Gulev SK, Hasse L (1999) Changes in wind waves in the North Atlantic over the last 30 years. Int J Climatol 19:1091–1117

Hanson JL, Tracy BA, Tolman HL, Scott DR (2009) Pacific hindcast performance of three numerical wave models. J Atmos Oceanic Technol 26(8):1614–1633

Harold JM, Bigg GR, Turner J (1999) Mesocyclone activity over the Northeast Atlantic. Part 2: an investigation of causal mechanisms. Int J Climatol 19(12):1283–1299

Hawkes PJ, Bagenholm C, Gouldby BP, Ewing J (1997) Swell and bimodal wave climate around the coast of England and Wales. Report SR 409, HR Wallingford

Hollweg H-D, Fast I, Hennemuth B, Keupthiel E, Lautenschlager M, Legutke S (2008) Ensemble simulations over Europe with the regional climate model CLM forced with IPCC AR4 global scenarios. M&D Technical Report No. 3, Hamburg

Holthuijsen LH (2007) Waves in oceanic and coastal waters. Cambridge University Press, Cambridge, p 404

IPCC AR4 (2007) Climate change 2007. Fourth assessment report of the intergovernmental panel on climate change. Cambridge University Press, Cambridge

IPCC SRES (2000) Special report on emissions scenarios (SRES). A special report of working group III of the intergovernmental panel on climate change. Cambridge University Press, Cambridge, p 559

Kaas E, Andersen U (2000) Scenarios for extra-tropical storm and wave activity: methodologies and results. ECLAT-2 blue workshop, climate scenarios for water related and coastal impact. KNMI, Netherlands

Kaas E, Andersen U, Flather RA, Willimas JA, Blackman DL, Lionello P, Dalan F, Elvini E, Nizzero A, Malguzzi P, Pfizenmayer A, von Storch H, Dillingh D, Phillipart M, de Ronde J, Reistad M, Midtbø KH, Vignes O, Haakenstad H, Hackett B, Fossum I, Sidselrud L (2001) Synthesis of the STOWASUS-2100 project: regional storm, wave and surge scenarios for the 2100 century. Danish Climate Centre Report 01–3. p 27

Kriezi EE, Broman B (2008) Past and future wave climate in the Baltic Sea produced by the SWAN model with forcing from the regional climate model RCA of the Rossby Centre. In: IEEE/OES US/EU-Baltic International Symposium (ed.), Tallinn, Estonia, 27–29 May 2008. pp 360–366

Li Y, Simmonds DJ, Reeve DE (2008) Quantifying uncertainty in extreme values of design parameters with resampling techniques. Ocean Eng 35(10):1029–1038

Lowe JA, Howard TP, Pardaens A, Tinker J, Holt J, Wakelin S, Milne G, Leake J, Wolf J, Horsburgh K, Reeder T, Jenkins G, Ridley J, Dye S, Bradley S (2009) UK climate projections science report: marine and coastal projections. Met Office Hadley Centre, Exeter

Mearns LO, Rosenweig C, Goldberg R (1997) Mean and variance change in climate scenarios: methods, agricultural applications, and measures of uncertainty. Clim Change 35:367–396

Muraleedharan G, Rao AD, Kurup PG, Unnikrishnan Nair N, Mourani S (2007) Modified Weibull distribution for maximum and significant wave height simulation and prediction. Coastal Eng 54(8):630–638

NCEP (2006). National Center for Environmental Prediction, Washington DC. Available at: http://polar.ncep.noaa.gov/waves/NEW-WAM.html

NGDC (2009). National Geophysical Data Centre. Available at: http://www.ngdc.noaa.gov/mgg/global/global.html

Padilla-Hernádez R, Perrie W, Toulany B, Smith PC, Zhang W, Jimenez-Hernández S (2004) Intercomparison of modern operational wave models. In: 8th International workshop on wave hindcasting and forecasting, North Shore, Oahu, Hawaii

Pryor SC, Barthelmie RG, Kjellström E (2005) Potential climate change impact on wind energy resources in northern Europe: nalyses using a regional climate model. Climate Dyn 25:815–835

Räisänen J, Hansson U, Ullerstig A, Döscher R, Graham LP, Jones C, Meier M, Samuelsson P, Willén U (2003) GCM driven simulations of recent and future climate with the Rossby Centre coupled atmosphere—Baltic Sea regional climate model RCAO. RMK No.101, Rossby Centre, SMHI

Räisänen J, Hanson U, Ullerstig A, Döscher R, Graham LP, Jones C, Meier HEM, Samuelsson P, Willén U (2004) European climate in the late twenty-first century: regional simulations with two driving global models and two forcing scenarios. Climate Dyn 22:13–31

Roeckner, Baeuml G, Bonaventura L, Brokopf R, Esch M, Giorgetta M, Hagemann S, Kirchner I, Kornblueh L, Manzini E, Rhodin A, Schlese U, Schulzweida U, Tompkins A (2003) The atmospheric general circulation model ECHAM 5. PART I: model description. MPI-Report 349

Sotillo M, Ratsimandresy A, Carretero J, Bentamy A, Valero F, Gonzalez-Rouco F (2005) A high-resolution 44-year atmospheric hind-cast for the Mediterranean basin: contribution to the regional improvement of global reanalysis. Climate Dyn 25 (2–3):219–236

Thompson P, Reeve DE, Stander J, Cai Y (2009) Automated threshold selection methods for extreme wave analysis. Coastal Eng 56 (10):1013–1021

Tolman (2002a) User manual and system documentation of WAVEWATCH-III version 2.22. NCEP/NOAA/NWS, National Center for Environmental Prediction, Technical note 222, Washington

Tolman HL (2002b) Validation of WAVEWATCH III version 1.15 for a global domain. NCEP/NOAA/NWS, National Center for Environmental Prediction, Technical note 213, Washington

Tolman HL (2003) Treatment of unresolved islands and ice in wind wave models. Ocean Model 5:219–231

van Heteren J, Bruinsma J (1981) A method to calculate the probability of exceedance of the design wave height. Coastal Eng 5:83–91

van Ulden AO, van Oldenborgh GJ (2006) Large-scale atmospheric circulation biases and changes in global climate model simulations and their importance for climate change in Central Europe. Atmos Chem Phys 6:863–881

van Ulden A, Lenderink G, van den Hurk B, van Meijgaard E (2007) Circulation statistics and climate change in Central Europe: PRUDENCE simulations and observations. Clim Change 81:179–192

WAMDI (1988) The WAM model—a third generation ocean wave prediction model. J Phys Oceanogr 18:1775–1810

Wang XLL, Swail VR (2006) Climate change signal and uncertainty in projections of ocean wave heights. Climate Dyn 26(2–3):109–126

Wang XLL, Zwiers FW, Swail VR (2004) North Atlantic Ocean wave climate change scenarios for the twenty-first century. J Climate 17(12):2368–2383

WASA (1998) Changing waves and storms in the Northeast Atlantic? Bull Am Meteorol Soc 79:741–760

WDCC (2009). World Data Centre for Climate, CERA-DB. Available at: http://cera-www.dkrz.de/

Winterfeldt J, Weisse R (2009) Assessment of value added for surface marine wind speed obtained from two regional climate models. Mon Weather Rev 137:2955–2965

WMO (1998) Guide to wave analysis and forecasting. WMO-No. 702. Secretariat of the world meteorological organization, Geneva, Switzerland